M. Abdalla & M. Skipper
ASR Corporation, 7817 Bursera NW, Albuquerque, NM 87120

D.V. Giri
Pro-Tech, 11-C Orchard Court, Alamo, CA 94507-1541

H. LaValley, T. Smith & D. McLemore
ITT Industries, AE&S Division, 6400 Uptown Blvd., NE, #300E, Albuquerque, NM 87110

J. Burger, R. Torres, T. Tran, W. Prather and C. E. Baum
Air Force Research Laboratory/DEHE, 3550 Aberdeen Ave SE, Kirtland AFB, NM87117

15 April 2001

Prototype IRA Memos

Memo 8

Evaluation of the Terminating Impedance in the Conical-Line Feed of the 6-foot IRA

Abstract

This memo describes the evaluation of the terminating impedance in the conical-line feed of the 6-foot IRA. The termination consists of series-parallel combination of lumped resistors. The capacitance of the termination is optimized via TDR (time-domain reflectometry) measurements.

1. Introduction

The 6-foot IRA that has been built and tested was described in [1]. In this memo, we describe the evaluation of the terminating impedance via TDR measurements.

2. 6-Foot IRA

This IRA system has the following major dimension and parameters:

$D \equiv$ Diameter of the reflector = 1.83m

$F \equiv$ focal length of the reflector = 0.685m

$f_d \equiv (F/D) = 0.343$ nearly the same as 12-foot IRA [2-5]

$Z_c^{(TEM)} \equiv$ (one line) $\simeq 400\ \Omega$ (nominal)

$Z_o \equiv$ characteristic impedance of free space $\simeq 376.98\ \Omega$

$f_g \equiv$ geometric factor (one line) $= Z_c^{(TEM)} / Z_o = 1.06$

Since the TEM characteristic impedance of each of the two transmission lines is 400 Ω, nominally one needs to terminate the lines in 400 Ω or 200 Ω between each of the 4 launcher plates and the reflector at its rim. There may be a "fine tuning" of this resistance needed to balance the electric and magnetic dipole moments of the IRA [6] at low frequencies. For the present, we have no easy way to monitor the low frequency performance of the IRA. In the future one may use the following considerations, to monitor the low frequency performance.

a) At low frequencies, an optimal radiation pattern is a cardioid with a maximum on forward axis (+z) and a null on reverse axis (-z) behind the reflector. Consequently, one can balance the dipole moments by measuring the backward radiation at low frequencies.
b) One could also make a long-time record of the radiated waveform on boresight and then optimize the low-frequency content of the radiated spectrum.

Owing to the limitations of available space and instrumentation, we could not monitor the low-frequency performance by tuning the terminating resistance. However,

the reactive part of the termination can be optimized via TDR measurements while maintaining the resistive part equal to TEM-characteristic impedance.

3. TDR Measurements

The experimental set-up for the TDR measurements is shown in figure 1. The actual test assembly is shown in figure 2, while the feed point details are shown in figure 3. The TDR head (SD-24) in a Tektronix scope 11801A is used as the input pulse and it is shown in figure 4. The TDR data for the cable, leading up to the antenna feed point is shown in figure 5, with the antenna disconnected. The TDR measurement with the cable and the antenna is shown in figure 6.

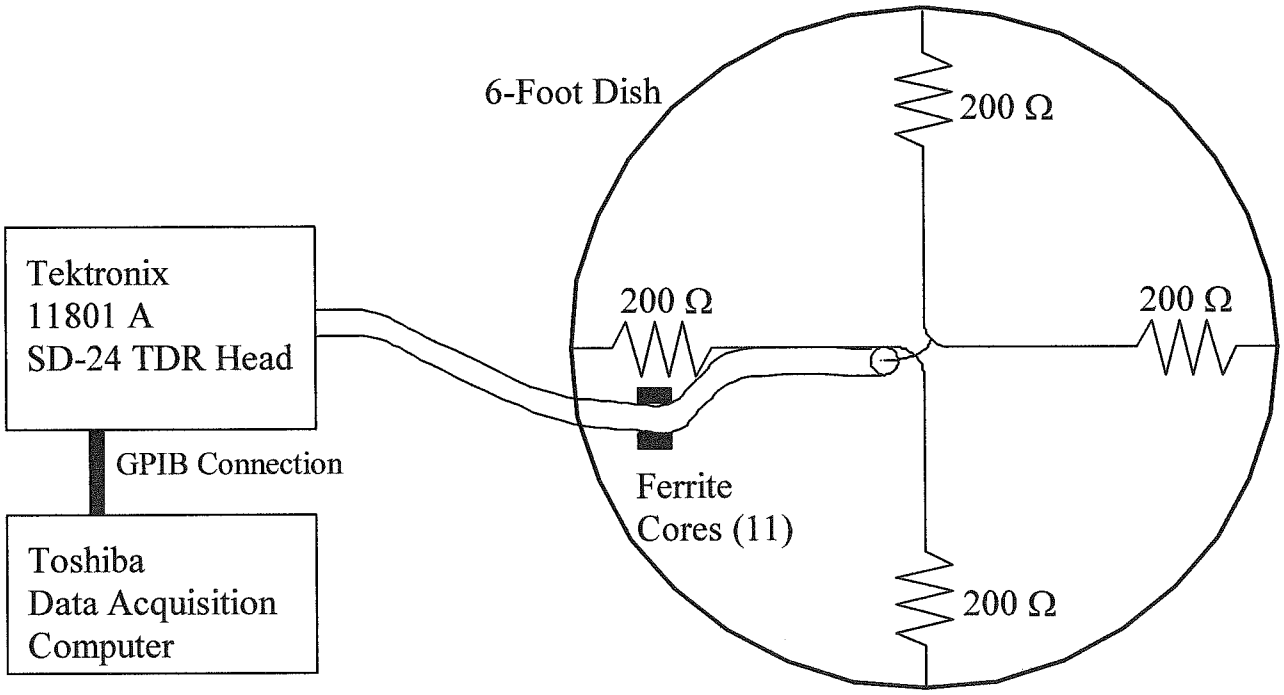

Figure 1. Schematic Diagram of Test Assembly

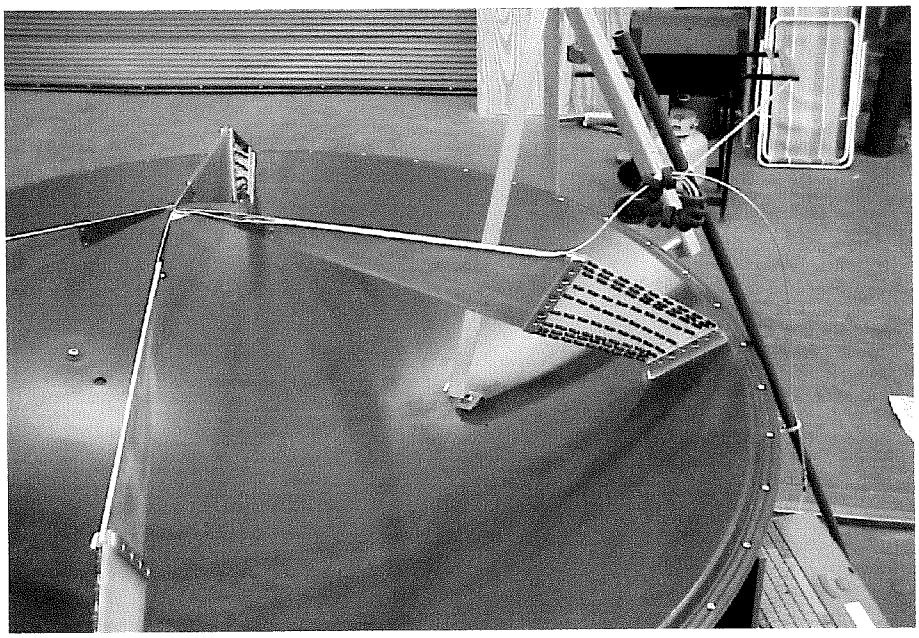

Figure 2. TDR Test Assembly

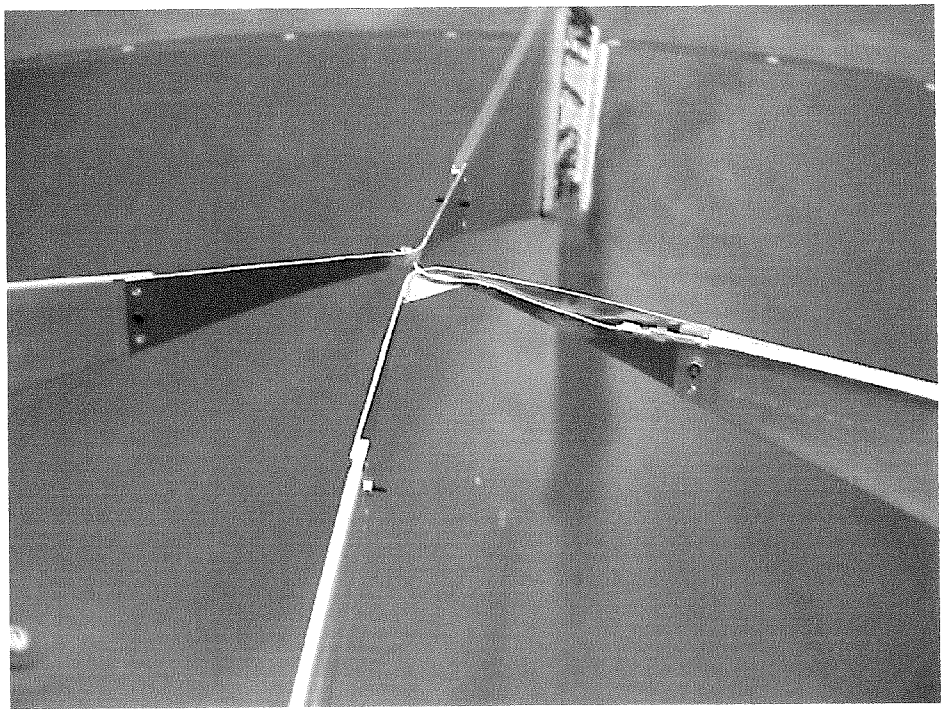

Figure 3. Feed-Point Detail

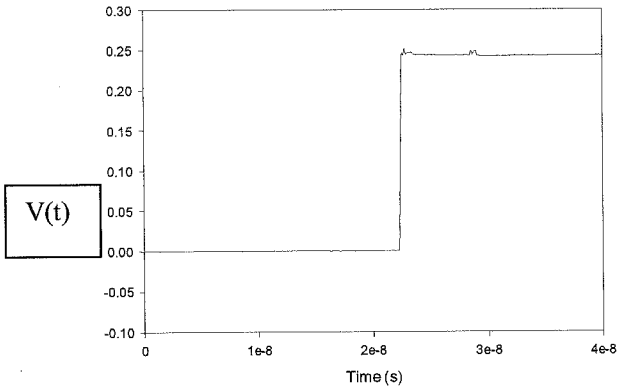

Figure 4. Input pulse for TDR measurements

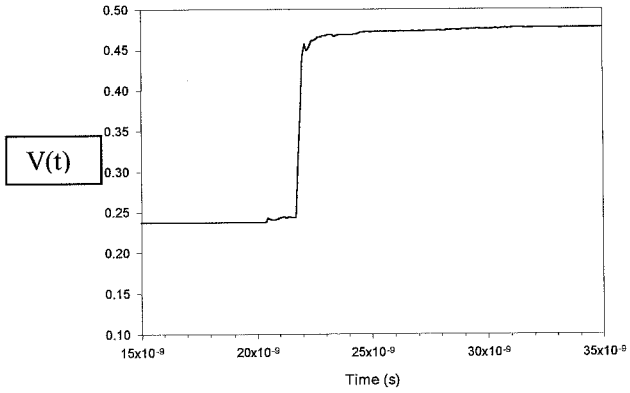

Figure 5. TDR of drive cable with the antenna disconnected (open cable)

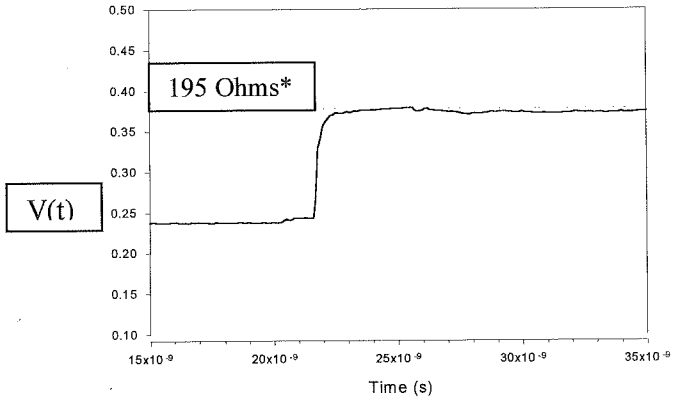

*** NOTE:**

We expect this to be closer to 200 Ohms and this suggests that the cable loss and dispersion might be the cause.

Figure 6. TDR Data for the 6-Foot IRA acquired with a 200 Ohm termination

From the TDR Data for the actual antenna system of the 6-foot IRA (shown in figure 6), one can see a small capacitive dip, at the beginning of the termination. The TDR data in figure 6 indicates an antenna input impedance of 195 Ω, which is within 3 % of the design value of 200 Ω.

4. Corrections to the Measured TDR to account for the Drive Cable

It is observed that the drive cable connecting the TDR instrument to the antenna feed point and the overall bandwidth of measurement influence the measurement and the measured data can be processed for this [7 and 8]. While noting that there are several ways one can process the measured data, we attempted the following simple procedure.

Numerical Procedure 1:

Step 1: $V_{input}(t)$ of figure 4 is Fourier transformed to get $\tilde{V}_{input}(f)$

Step 2: The reflected pulse component of $V_{cable}(t)$ of figure 5 is Fourier transformed to get $\tilde{V}_{cable}(f)$

Step 3: The impulse response $\tilde{V}_{imp}(f)$ is obtained by computing $\tilde{V}_{input}(f) \,/\, \tilde{V}_{cable}(f)$

Step 4: The reflected pulse component of $V_{antenna}(t)$ of figure 6 is Fourier transformed to get $\tilde{V}_{antenna}(f)$

Step 5: $\tilde{V}_{cor}(f)$ is obtained by computing $\tilde{V}_{antenna}(f) \,/\, \tilde{V}_{imp}(f)$

Step 6: $V_{cor}(t)$, which is the corrected antenna TDR, is obtained by Fourier inverting $\tilde{V}_{cor}(f)$ and adding the incident pulse.

However, we had numerical difficulties in Fourier transforming time domain waveforms that do not return to zero. There are many ways to get around this problem and we chose to process the data as indicated below:

Numerical Procedure 2:

Step 1: $V_{input}(t)$ of figure 4 is differentiated and then Fourier transformed to get $j\omega\, \tilde{V}_{input}(f)$

Step 2: The reflected pulse component of $V_{cable}(t)$ of figure 5 is differentiated and then Fourier transformed to get $j\omega \tilde{V}_{cable}(f)$

Step 3: The impulse response $\tilde{V}_{imp}(f)$ is obtained by computing

$$j\omega \tilde{V}_{input}(f) \;/\; j\omega \tilde{V}_{cable}(f)$$

Step 4: The reflected pulse component of $V_{antenna}(t)$ of figure 6 is first differentiated and then Fourier transformed to get $j\omega \tilde{V}_{antenna}(f)$

Step 5: $j\omega \tilde{V}_{cor}(f)$ is obtained by computing $j\omega \tilde{V}_{antenna}(f) \;/\; \tilde{V}_{imp}(f)$

Step 6: $V_{cor}(t)$, which is the corrected antenna TDR, is obtained by Fourier inverting $j\omega \tilde{V}_{cor}(f)$, then integrating this waveform and adding the incident pulse.

Step 7: $V_{filter}(t)$, which is the corrected antenna TDR with filtering, is obtained by Fourier inverting $j\omega \tilde{V}_{cor}(f)$, passing it through a low-pass filter (6 GHz), Fourier inverting, integrating the resultant time domain waveform and adding the incident pulse.

The results of numerical procedure 2, outlined above are shown in figures 7 and 8.

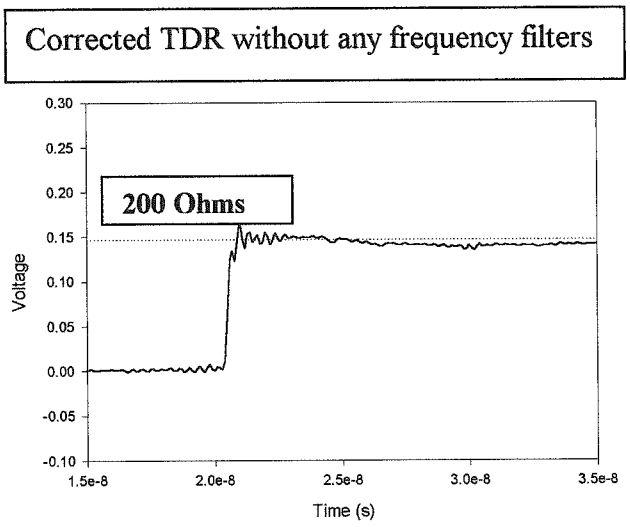

Figure 7. Corrected TDR data for the 6-foot IRA, without filtering out any frequencies

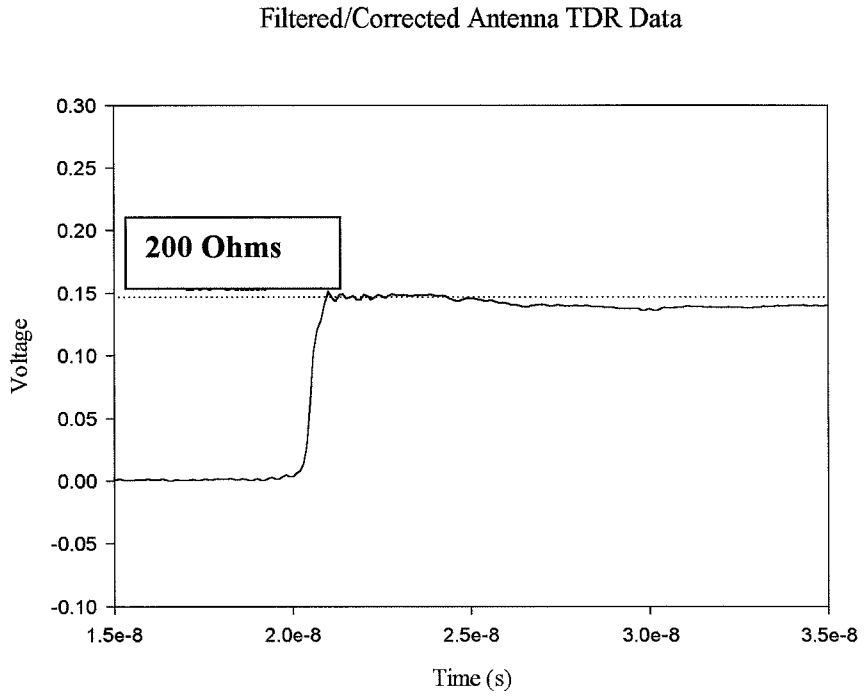

Figure 8. Corrected TDR data for the 6-foot IRA, after filtering out all frequencies above 6 GHz.

In the unfiltered results of figure 7, it is observed that there is a rippling waveform that is a very high-frequency signal, which is recognized to be a numerical artifact. The measurement system is band-limited and hence the use of a low pass filter with a cut-off frequency of 6 GHz has been used resulting in the corrected TDR waveform of figure 8 kabove. Noisy data was observed above 6 GHz in Fourier transformed waveforms. The low-pass filter used is characterized by a single-pole, with a 3 dB point at 6 GHz. The corrected waveform of figure 8 displays an antenna impedance of nearly 200 Ohms, and the capacitive component in the terminator is still present, indicating further improvement may still be possible.

5. Energy and Voltage Stand-off in the Terminator

For an approximately double exponential input pulse, the energy available at the terminator is given by:

$$U_t \simeq \frac{Vo^2}{2bZ_L}$$

letting conservatively Vo = 80 kV (The full voltage is $\pm$ 80 kV), b^{-1} = 20ns and $Z_L \simeq 200$ Ω, U_T is of the order of 0.32 J. There appears to be no problem in dissipating this energy in a single pulse.

We have used 9 parallel chains, 8 series resistors in each chain. The voltage drop across each resistor is < 20 kV. One Watt Allen-Bradley carbon composite resistors can withstand this voltage drop for the duration of the pulse. When the pulser is operated at a repetition rate of 400 Hz, the average power is estimated to be:

$$P_{avg} = \frac{V^2}{R} \text{ x pulse duration x prf}$$

$$= \frac{(80kV)^2}{200} \text{ x } 20ns \text{ x } 400Hz$$

$$\approx 255 \text{ Watts}$$

With 8 resistors in series per chain and 9 chains, we have a power dissipation of (255/72) = 3.5 Watts per resistor. The 3.5 Watts per resistor is the average power dissipated in each resistor, for a square pulse. For an exponentially decaying pulse, we find that Allen-Bradley (carbon composition) resistors rated for 1 or 2 Watts are adequate.

6. Summary

Conical Lines that feed the reflector have been terminated in its TEM characteristic impedance, which are purely resistive. The reactive component has been optimized via TDR measurements.

References

1. B. Cockreham, F.R. Gruner, D.V. Giri, H. LaValley, T. Smith, D. McLemore, J. Burger, R. Torres, T. Tran, W. Prather and C. E. Baum, "Fabricational Details of the 6-Foot IRA," Prototype IRA Memo 7, 1 April 2001.

2. D.V. Giri and H. Lackner, "Fabricational Details of Prototype IRAs," Prototype IRA Memo 1, 1 May 1994.

3. D.V. Giri and H. Lackner, "Preliminary Evaluation of the Terminating Impedance in the Conical-Line Feed of IRAs," Prototype IRA Memo 2, 15 May 1994.

4. D.V. Giri and H. Lackner, "Estimates of Peak Values of Near and Far Fields of Prototype IRAs," Prototype IRA Memo 4, 15 May 1994.

5. D.V. Giri, H. Lackner, I.D. Smith, D.W. Morton, C.E. Baum, J.R. Mavek, D. Scholfield and W.D. Prather, "A Reflector Antenna for Radiating Impulse-Like Waveforms," Sensor and Simulation Note 382, 4 July 1995.

6. D.V. Giri and S.Y. Chu, "On the Low-Frequency Electric Dipole Moment of Impulse Radiating Antennas (IRAs)," Sensor and Simulation Note 346, October 1992.

7. N. S. Nahman, " Software Correction of Measured Pulse Data", **Fast Electrical and Optical Measurements,** edited by J. E. Thompson and L. H. Luessen, NATO Advanced Science Institutes Series, Martinus Nijhoff Publishers, pp 351-417.

8. P. E. Patterson, "The Complete Fast Fourier Transform and Cascaded Transition-Band Filters to reduce the Noise of Deconvolution", Measurement Note 56, January 2001.